The British Journal of Radiology, 85 (2012), 897–904

Multidetector CT features of pulmonary focal ground-glass opacity: differences between benign and malignant

L FAN, MD, S-Y LIU, MD, Q-C LI, MD, H YU, MD and X-S XIAO, MD

Department of Radiology, Changzheng Hospital, Second Military Medical University, Shanghai, China

Objective: To evaluate different features between benign and malignant pulmonary focal ground-glass opacity (fGGO) on multidetector CT (MDCT).
Methods: 82 pathologically or clinically confirmed fGGOs were retrospectively analysed with regard to demographic data, lesion size and location, attenuation value and MDCT features including shape, margin, interface, internal characteristics and adjacent structure. Differences between benign and malignant fGGOs were analysed using a χ^2 test, Fisher's exact test or Mann–Whitney *U*-test. Morphological characteristics were analysed by binary logistic regression analysis to estimate the likelihood of malignancy.
Results: There were 21 benign and 61 malignant lesions. No statistical differences were found between benign and malignant fGGOs in terms of demographic data, size, location and attenuation value. The frequency of lobulation ($p=0.000$), spiculation ($p=0.008$), spine-like process ($p=0.004$), well-defined but coarse interface ($p=0.000$), bronchus cut-off ($p=0.003$), other air-containing space ($p=0.000$), pleural indentation ($p=0.000$) and vascular convergence ($p=0.006$) was significantly higher in malignant fGGOs than that in benign fGGOs. Binary logistic regression analysis showed that lobulation, interface and pleural indentation were important indicators for malignant diagnosis of fGGO, with the corresponding odds ratios of 8.122, 3.139 and 9.076, respectively. In addition, a well-defined but coarse interface was the most important indicator of malignancy among all interface types. With all three important indicators considered, the diagnostic sensitivity, specificity and accuracy were 93.4%, 66.7% and 86.6%, respectively.
Conclusion: An fGGO with lobulation, a well-defined but coarse interface and pleural indentation gives a greater than average likelihood of being malignant.

Received 22 August 2010
Revised 14 March 2011
Accepted 17 March 2011

DOI: 10.1259/bjr/33150223

With the availability of low-dose spiral CT scan of the lung, focal ground-glass opacity (fGGO) that was difficult to detect on conventional chest radiographs has increasingly been detected [1–3]. Ground-glass opacity (GGO) is defined as an area of a slight homogeneous increase in density, which does not obscure underlying bronchial structures or vascular margins on high-resolution CT (HRCT) [4]. Pathologically, GGO may be caused by partial airspace filling, interstitial thickening with inflammation, oedema, fibrosis, neoplastic proliferation, the normal respiratory condition or increased pulmonary capillary blood volume [5]. GGO can be classified as pure GGO (pGGO) or mixed GGO (mGGO) based on the presence of solid components. Although GGO is a common and non-specific finding of lung HRCT, and may occur in benign lung conditions such as organising pneumonia, focal fibrosis and haemorrhage [6–8], it has recently received considerable attention because it may indicate an early underlying lung cancer, which in most cases presents as bronchioloalveolar carcinoma (BAC) and adenocarcinoma with a predominant BAC component. It was reported in a study [9] that 17 of 28 pGGOs were BAC, 3 were adenocarcinoma and 8 were atypical adenomatous hyperplasia (AAH). Several other studies [10, 11] have also indicated that mGGOs are more likely to be malignant, with the malignant rate of pGGO and mGGO being 18% and 63%, respectively [12]. The aim of the present study was to retrospectively compare the features of benign and malignant fGGOs on thin section multidetector CT (MDCT) images in an attempt to identify characteristics that would help the differential diagnosis of fGGOs.

Address correspondence to: Dr Shi-yuan Liu, Department of Radiology, Changzheng Hospital, Second Military Medical University, No. 415 Fengyang Road, Shanghai 200003, China. E-mail: lsy0930@163.com

This work was funded by the Natural Science Foundation of Shanghai (no. 10ZR1438900), the Youth Fund of the National Natural Science Foundation of China (no. 81000602), the ''Mountaineering plan'' Major Subject Program of the Science and Technology Committee of Shanghai (no. 06DZ19503), the Major Subject Program of the Science and Technology Committee of Shanghai (no. 08DZ1900707) and National the Natural Science Foundation of China (no. 30970800).

Methods and materials

Patient population

From January 2007 to April 2010, a consecutive series of 84 fGGO lesions of ≤4 cm in diameter were found on CT

in 84 patients in our institution. Of them, 82 fGGOs in 82 patients that had been confirmed by operative pathology (n=57), biopsy pathology (n=12) or clinical diagnosis (n=13) by June 2010 were used for retrospective analysis in this study. The clinical diagnosis was based on a significant reduction in size or complete disappearance of the lesion on follow-up MDCT images after anti-inflammatory therapy. The other two lesions were excluded from the present study owing to their equivocal nature (*i.e.* that they have remained stable during the follow-up period until now). Of the 82 fGGOs enrolled, 61 were diagnosed as malignant, comprising adenocarcinoma (26), BAC (33), large-cell lung cancer (1) and adenosquamous carcinoma (1); and the remaining 21 were diagnosed as benign, comprising inflammation (14), organising pneumonia (1), focal fibrosis (2) and AAH (4). Definite histological or clinical diagnosis of these 82 fGGOs was obtained within 6 months. The local ethics committee approved this retrospective study and waived informed consent.

Image acquisition

All the patients were scanned on a 16-MDCT scanner (Acquilion 16; Toshiba, Tokyo, Japan). Breath-hold training was carried out before each examination. All subjects were asked to hold their breath at the end of inspiration for as long as possible. A non-enhanced scan was performed from the thoracic inlet to the middle portion of the kidneys, followed by contrast-enhanced scan of the lesion area only in arterial and delayed phases, to reduce exposure to radiation. For contrast-enhanced scans, all injections were performed with an automatic power injector, with which 90 ml contrast medium (Optiray 350 mgI ml^{-1}; Mallinckrodt Medical, St Louis, MO) was injected into the antecubital vein at a rate of 4 ml s^{-1}. Arterial phase and delayed phase images were acquired at 20–25 s and 90 s after injection, respectively [13]. The imaging parameters were as follows: 250 mA, 120 kVp, collimation 1 mm, pitch 0.98 and filtration coefficient 52 or 1 (high- or standard-resolution algorithms).

Demographic data and image analysis

Patients' demographic data included sex and age. All the raw data sets were sent to a Vitrea 1 workstation and reconstructed. Reconstruction for axial images was performed with a section thickness of 1 mm, a reconstruction interval of 0.8 mm, field of view (FOV) of approximately 18×18 cm to 20×20 cm and a filtration coefficient of 52 or 1, and was viewed at the mediastinal and pulmonary window settings. Multiplanar reconstructions (MPRs) and three-dimensional volume-rendered (VR) images were then performed to display the morphological features and relationships with the adjacent bronchi and vessels.

All the post-processed images were interpreted by two thoracic radiologists with 15 and 10 years' experience in chest CT. The observers were blinded to the subjects' identities and clinical data. Decisions on CT findings were reached by consensus. CT scans were assessed by observing lesion location, size, shape, margin, interface, internal characteristics, adjacent structure and attenuation value. Lesion size was defined as the longest dimension. Shape was classified as irregular or round/oval. Marginal characteristics included lobulation, spiculation, cusp angle and spine-like process. Cusp angle and spine-like process were both defined as a structure extending from the lesion, while their borders with lung parenchyma were different: cusp angle with either straight or slightly concave borders, and spine-like process with at least one convex border. Interfaces were classified as one of three types: ill-defined, well-defined and smooth, and well-defined but coarse. Internal characteristics included air bronchograms and other air-containing space. Air bronchograms were classified as natural, dilated and distorted, or cut-off. The definition of a natural air bronchogram was running naturally with the regular bronchial wall [14]. Findings of adjacent structures included the pleural indentation sign and the vascular convergence sign. For mGGO, attenuation values of the GGO component, solid component and adjacent parenchyma on non-enhanced scan were recorded, and those of the solid component on contrast-enhanced scan were also recorded. For pGGO, attenuation values of the GGO and adjacent parenchyma were recorded only on non-enhanced scan. Then, the difference in attenuation value between the GGO component and adjacent parenchyma was calculated. A region of interest (oval or circular) covering one-half to two-thirds of the largest area in a lesion away from air-containing space was selected.

Statistical analysis

The statistical analysis of all data sets was performed with SPSS v.11.0 software (SPSS Inc., Chicago, IL). The sex ratio of the patients and the morphological features of the lesions were analysed for differences between benign and malignant fGGOs using the χ^2 test or Fisher's exact test. Patient age, lesion size and attenuation value were analysed with the Mann–Whitney U-test. A two-sided value of $p<0.05$ was used as the criterion to indicate a statistically significant difference.

In addition, binary logistic regression analysis was performed on the morphological characteristics to draw a regression equation to estimate the likelihood of malignancy. The forward conditional method was employed for variable selection.

Results

Demographic data, lesion size and location

With respect to the demographic data of the 82 patients (35 males, 47 females; mean age, 59.02±9.63 years; age range, 40–84 years), there was no significant difference in either the sex ratio (p=0.120) or age (p=0.648) between patients with benign and malignant fGGOs. Also, there was no significant difference in either lesion size (mean size, 2.35±0.72 cm; size range, 0.5–4 cm, p=0.955) or location (p=0.902) between benign and malignant fGGOs (Table 1).

Table 1. Demographic data, nodule size and location of benign and malignant focal ground-glass opacity (fGGO)

fGGO	Benign (n=21)	Malignant (n=61)	p-value
Sex ratio (M:F)	12:9	23:38	0.120[a]
Average age (years)	60.5±11.07	58.68±9.39	0.648[b]
Average size D (cm)	2.33±0.71	2.36±0.73	0.955[b]
Location			
RUL	10	21	0.902[c]
RML	2	7	
RLL	3	10	
LUL	4	13	
LLL	2	10	

D, longest dimension; F, female; LLL, left lower lobe; LUL, left upper lobe; M, male; RLL, right lower lobe; RML, right middle lobe; RUL, right upper lobe.
Sex ratio and location are expressed in terms of frequency; age and size are expressed as mean ± standard deviation.
[a]χ^2 test.
[b]Mann–Whitney *U*-test.
[c]Fisher's exact test.

Attenuation values

The fGGOs included 68 lesions with mGGO appearance and 14 with pGGO appearance. For the solid component of the mGGOs, the mean CT attenuation values on non-enhanced CT images (p=0.520), on arterial phase images (p=0.464) and on delayed phase images (p=0.869) were not significantly different between benign and malignant mGGOs. For the difference in attenuation value between the GGO component and the adjacent parenchyma on non-enhanced CT images, there was no significant difference between benign and malignant mGGOs or pGGOs, the corresponding p-values being 0.068 and 1.000, respectively (Table 2).

Comparison of morphological features between benign and malignant fGGOs

Of the 21 benign fGGOs, 14 were mGGOs and 7 were pGGOs. Of the 61 malignant fGGOs, 54 were mGGOs and 7 were pGGOs. Statistically significant difference was found between benign and malignant fGGOs in the frequency of lobulation (14.3 *vs* 83.6, p=0.000; Figure 1), spiculation (4.8 *vs* 34.4, p=0.008; Figure 2), spine-like process (0 *vs* 29.5, p=0.004; Figure 3), ill-defined interface (66.7 *vs* 1.6, p=0.000; Figure 4), well-defined but coarse interface (33.3 *vs* 93.4, p=0.000; Figure 2), air-containing space (14.3 *vs* 59.0, p=0.000; Figure 5), pleural indentation (4.8 *vs* 70.5, p=0.000; Figure 1) and vascular convergence (4.8 *vs* 36.1, p=0.006; Figure 1) (Table 3). In terms of air bronchograms, there was no significant difference between benign and malignant fGGOs in the incidence of either natural (p=0.502) or dilated and distorted (p=1.000) bronchus, while the incidence of cut-off was significantly different (0 *vs* 32.8, p=0.003; Figure 1). There was no significant difference between benign and malignant fGGOs in the incidence of other morphological characteristics such as shape, well-defined and smooth interface and cusp angle (Figure 6) (p>0.05).

Binary logistic regression analysis

In binary logistic regression analysis of the present study, benignity and malignancy were regarded as dependent variables, and the shape, lobulation, spiculation, cusp angle, spine-like process, interface, air bronchograms, other air-containing space, pleural indentation sign and vascular convergence were regarded as independent variables. The result showed that lobulation, interface and pleural indentation were important indicators for malignant diagnosis of fGGO; the corfresponding regression equation was as follows:

$$\ln(p/1-p) = -2.268 + 2.095 \times \text{lobulation} + 1.144 \times \text{interface} + 2.206 \times \text{pleural indentation}$$

where p is the probability of malignant fGGO. When the p-value was ≥0.5, the lesion was expected to be malignant, while the others were categorised as benign.

In terms of malignant fGGO diagnosis, the odds ratios (ORs) of lobulation, pleural indentation and interface were 8.122, 9.076 and 3.139, respectively (Table 4). In other words, the malignant risk of an fGGO with lobulation was 8.122 times that without lobulation; the malignant risk of an fGGO with pleural indentation was 9.076 times that without pleural indentation; the malignant risk of an fGGO with well-defined but coarse interface was 3.139 times that with well-defined and smooth interface; and the malignant risk of an fGGO with well-defined and smooth interface was 3.139 times that with ill-defined interface. It was evident that well-defined but coarse interface was the most important discriminator of the three interface types.

Table 2. Attenuation values of benign and malignant mixed ground-glass opacity (mGGO) and pure ground-glass opacity (pGGO)

fGGO	Component	Attenuation value (HU)		
		Benign	Malignant	p-value
mGGO	Solid component			
	Non-enhanced scan	37.57±9.34	38.75±7.79	0.520[b]
	Arterial phase	65.14±21.71	60.85±24.90	0.464[b]
	Delayed phase	80.00±23.09	79.55±24.91	0.869[b]
	GGO component[a]	482.57±144.13	341.93±198.26	0.068[b]
pGGO	GGO component[a]	210±54.06	314.5±62.55	1.000[b]

fGGO, focal ground-glass opacity.
Attenuation values are expressed as mean ± standard deviation.
[a]Difference of attenuation value between the GGO component and adjacent parenchyma.
[b]Mann–Whitney *U*-test.

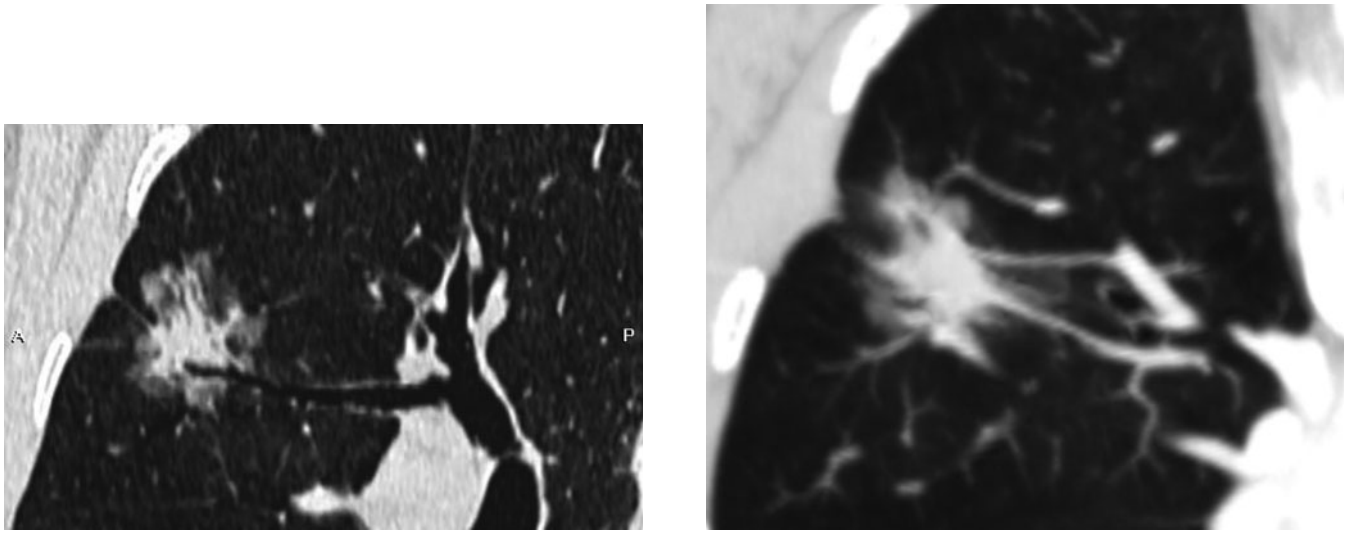

(a) (b)

Figure 1. Bronchioloalveolar cardnoma in a 62-year-old male. (a) Oblique multiplanar reconstruction lung window shows a 23 mm focal ground-glass opacity with lobulation and bronchus cut-off in the right upper lobe. (b) Maximum-intensity projection shows the vascular convergence sign and pleural indentation.

The probability of a malignancy was calculated for each lesion using the above-mentioned regression equation. Table 5 lists the numbers of expected diagnosis by the logistic regression equation (expected) and final pathological or clinical diagnosis by follow-up (observed) of benign and malignant fGGOs. Predictive values of the regression analysis were 14 and 57 for benign and malignant fGGO, respectively. Sensitivity, specificity and accuracy with this regression equation were calculated as 93.4%, 66.7% and 86.6%, respectively.

Binary logistic regression analysis of the morphological characteristics was also performed between benign and malignant mGGOs, and between benign and malignant pGGOs.

The results showed that lobulation and interface were important indicators for malignant diagnosis of mGGO; the

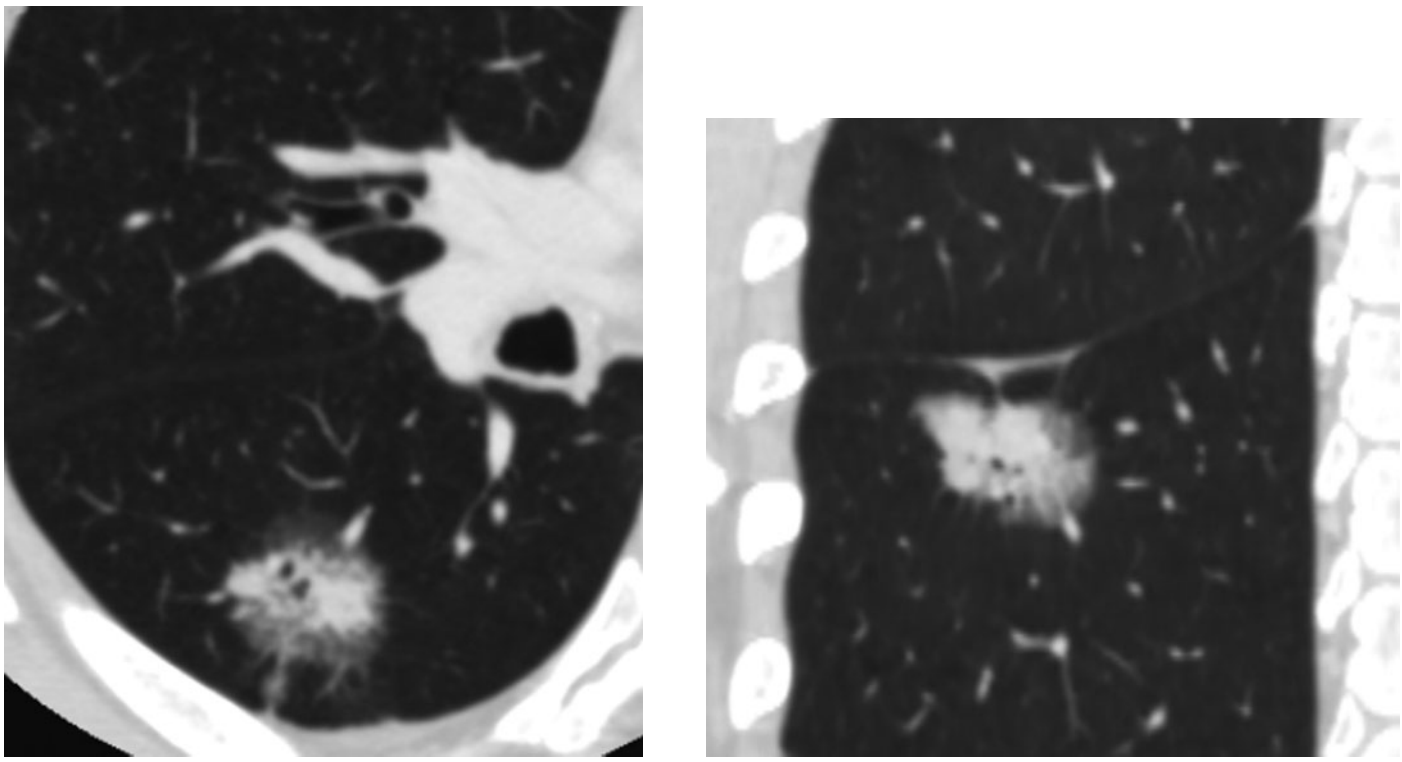

(a) (b)

Figure 2. Adenocarcinoma in a 54-year-old female. (a) Transverse lung window thin-section (1 mm thick) and (b) coronal multiplanar reconstruction show a 25 mm focal ground-glass opacity with spiculation and a well-defined but coarse interface in the right lower lobe.

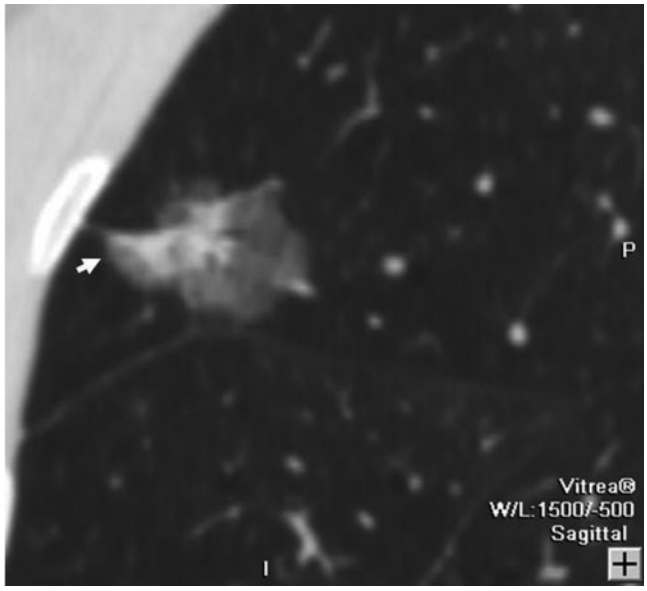

Figure 3. Bronchioloalveolar carcinoma in a 45-year-old female. Sagittal multiplanar reconstruction lung window shows a 28 mm focal ground-glass opacity with a spine-like process (arrow) in the right upper lobe.

regression equation was:

$$\ln(p/1-p) = -2.884 + 2.977 \times \text{lobulation} + 1.673 \times \text{interface}$$

In terms of malignant mGGO diagnosis, the ORs of lobulation and interface were 19.620 and 5.329, respectively. Sensitivity, specificity and accuracy were 98.1%, 57.1% and 89.7%, respectively.

The results of binary logistic regression analysis also showed that interface was the most important indicator for malignant diagnosis of pGGO; the regression equation was:

$$\ln(p/1-p) = -1.657 + 1.522 \times \text{interface}$$

The OR was 4.582 for the malignant pGGO diagnosis. Sensitivity, specificity and accuracy were calculated as 57.1%, 71.4% and 64.3%, respectively.

Discussion

Ever since spiral CT was used in lung cancer screening, small peripheral or early-stage lung cancers have been detected more frequently. Histologically, most of these lung cancers are well-differentiated adenocarcinoma or BAC [1, 2, 6, 15], typically appearing as fGGOs on HRCT. About 30% of benign pulmonary lesions also manifest as fGGOs [16]. Although some studies have reported MDCT features of fGGO lesions [8, 17–19], the differential features between benign and malignant fGGOs still deserve to be investigated.

The binary regression analysis of our study revealed that lobulation, interface and pleural indentation were the most important discriminators between benign and malignant fGGOs. The corresponding regression equation for differential diagnosis of fGGOs yielded high sensitivity (93.4%) and accuracy (86.6%).

The marginal characteristics of pulmonary nodules usually reflect their underlying pathological nature. Lobulation is a common finding of lung MDCT and is more frequently seen in malignant than in benign

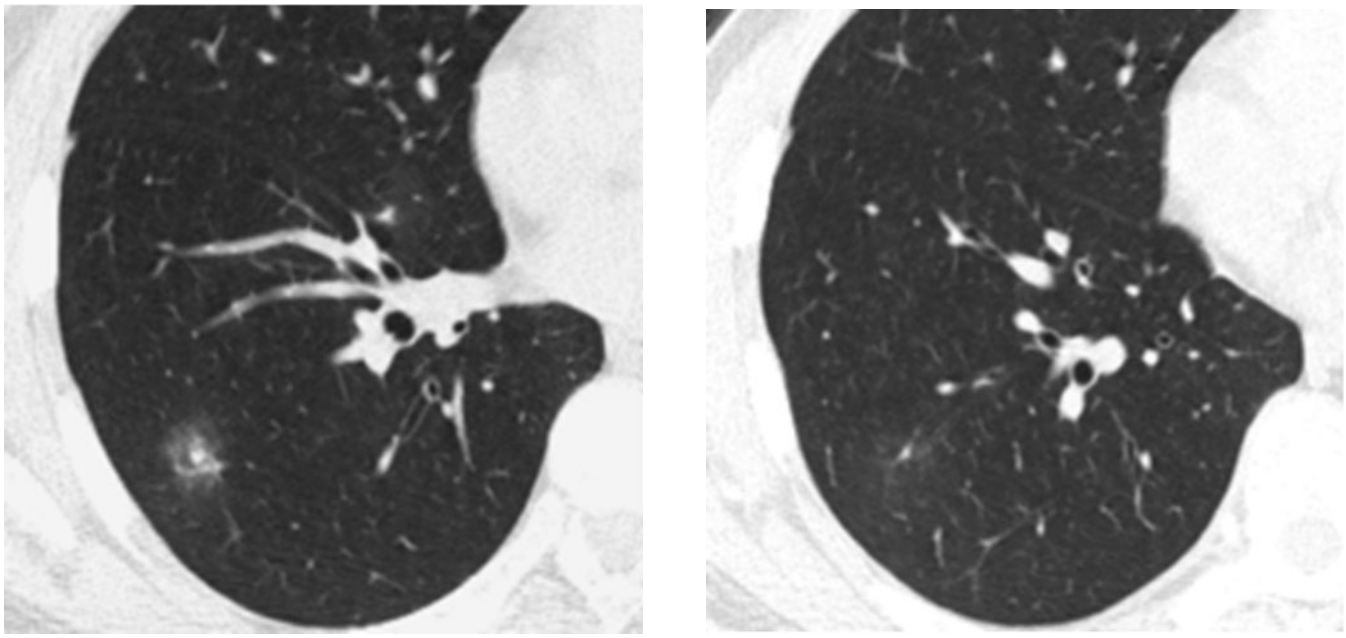

(a) (b)

Figure 4. An inflammatory lesion in a 53-year-old female. (a) Transverse lung window shows a focal ground-glass opacity with an ill-defined interface in the right lower lobe. (b) Transverse lung window shows that the lesion has almost disappeared after anti-inflammatory therapy.

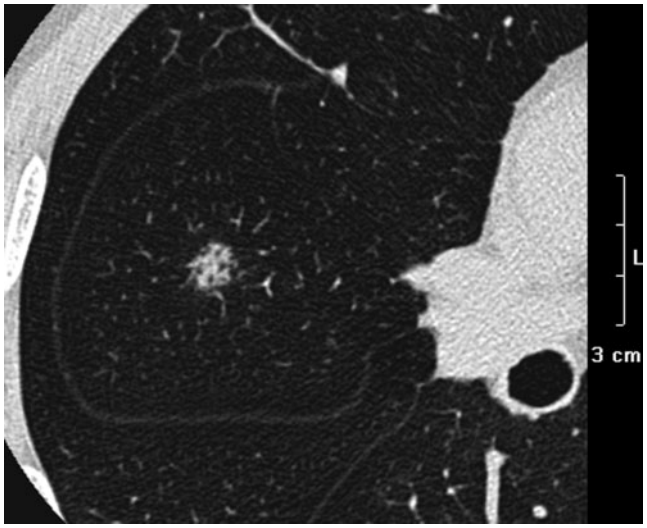

Figure 5. Adenocarcinoma in a 59-year-old male. Transverse lung window thin-section (0.5 mm thick) shows an 8 mm focal ground-glass opacity with air-containing space in the right middle lobe.

pulmonary lesions. Pathologically, malignant lobulation is caused by different growth velocity owing to different cell differentiation, tumour growth blocked by the adjacent pulmonary interstitium and contraction of fibrous tissue inside the lesion [5, 18, 20]. The pathological basis of benign lobulation is hyperplasia of connective tissue inside or around the nodules and cicatrical contraction [8, 20]. It was found in the present study that the frequency of lobulation in malignant fGGOs was significantly higher than in benign ones (83.6% *vs* 14.3%). The frequency of lobulation in malignant fGGOs was similar to that reported in another study [21], while the frequency of lobulation in benign fGGOs was lower. The reason may be due to the small sample size of benign fGGOs in this study.

Interface is another valuable discriminator for benign and malignant fGGOs. In the present study, we classified the interface as ill-defined, well-defined and smooth, and well-defined but coarse. The result of our binary regression analysis showed that a well-defined but coarse interface was the most important discriminator among the three types. In most cases of lung cancer, the interface is usually well defined but wholly or partially coarse, the pathological basis of which generally includes the following three aspects: an infiltrative tumour growth, inflammatory reaction in the peritumour parenchyma, and carcinomatous embolus formation in small vessels or lymph vessels [8, 18]. Of the three aspects, the tumour growth pattern is the most important. In the present study, except for one case with an ill-defined interface, all malignant cases appeared with a well-defined interface (57 coarse, 3 smooth). Conversely, the interface of benign lesions is usually ill defined owing to infiltration of inflammatory cells. Two-thirds (14/21) of the benign fGGOs in our series showed an ill-defined interface. The frequency of well-defined and smooth interface in benign and malignant fGGOs was very similar (p=0.566). It is pathologically caused by a stacking tumour growth or a pseudocapsule resulting from compression of the adjacent pulmonary parenchyma by fast tumour growth [19]. In our opinion, a well-defined but coarse interface is more suggestive of malignancy, while an ill-defined interface is more likely to be benign. Nambu et al [18] pointed out that a well-defined margin was a valuable discriminator for GGO.

Table 3. Distribution of morphological features in benign and malignant focal ground-glass opacity on mutidetector CT

	Benign (n=21)			Malignant (n=61)			
fGGO	mGGO	pGGO	Total 1	mGGO	pGGO	Total 2	p-value
Shape							
Irregularity	10	1	11 (52.4)	13	0	13 (21.3)	0.07[a]
Round/oval	4	6	10 (47.6)	41	7	48 (78.7)	
Margin							
Lobulation	2	1	3 (14.3)	48	3	51 (83.6)	0.000[a]
Spiculation	1	0	1 (4.8)	21	0	21 (34.4)	0.008[a]
Cusp angle	2	0	2 (9.5)	2	0	2 (3.3)	0.568[b]
Spine-like process	0	0	0 (0)	18	0	18 (29.5)	0.004[b]
Interface							
Ill defined	9	5	14 (66.7)	1	0	1 (1.6)	0.000[b]
Well defined, smooth	0	0	0 (0)	0	3	3 (4.9)	0.566[b]
Well defined, coarse	5	2	7 (33.3)	53	4	57 (93.4)	0.000[b]
Internal characteristics							
Air bronchograms							
Natural	3	2	5 (23.8)	9	0	9 (14.8)	0.502[b]
Dilated and distorted	3	0	3 (14.3)	9	0	9 (14.8)	1.000[b]
Cut-off	0	0	0 (0)	19	1	20 (32.8)	0.003[a]
Air-containing space	3	0	3 (14.3)	33	3	36 (59.0)	0.000[a]
Adjacent structure							
Pleural indentation	1	0	1 (4.8)	40	3	43 (70.5)	0.000[a]
Vascular convergence	1	0	1 (4.8)	22	0	22 (36.1)	0.006[a]

fGGO, focal ground-glass opacity; mGGO, mixed ground-glass opacity; pGGO, pure ground-glass opacity.
Data are expressed in terms of frequency or percentages (in parentheses).
[a] χ^2 test.
[b] Fisher's exact test.

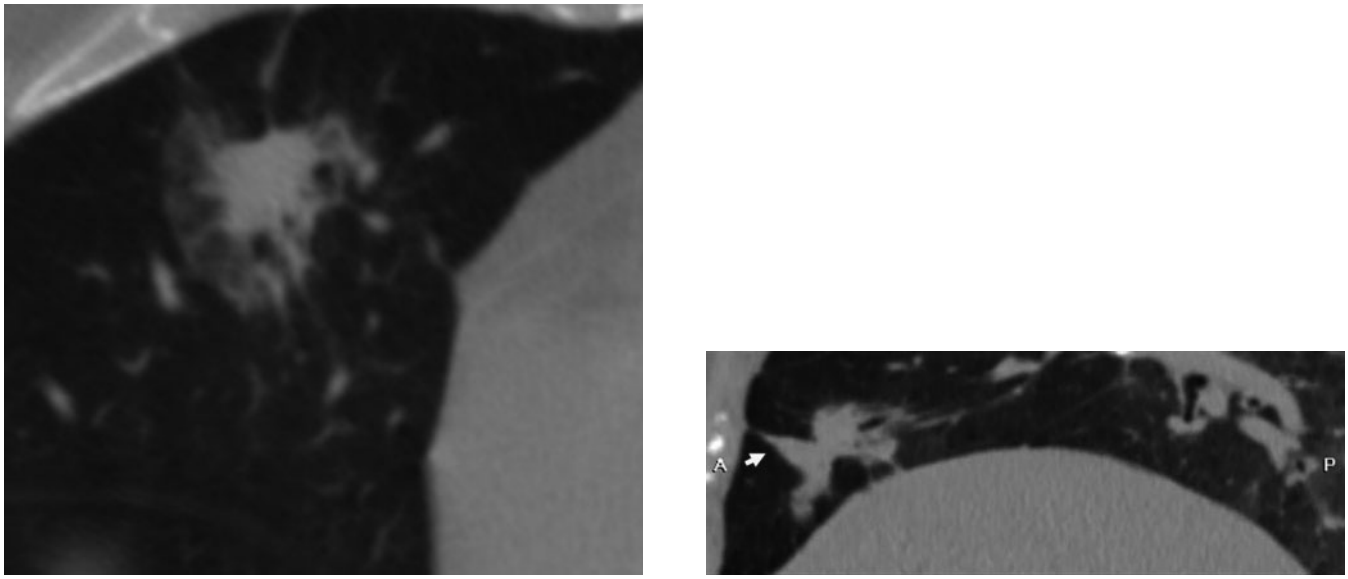

(a) (b)

Figure 6. An inflammatory lesion in a 75-year-old male. (a) Transverse lung window thin-section (1 mm thick) shows a 25 mm focal ground-glass opacity in the right middle lobe. (b) Sagittal multiplanar reconstruction shows cusp angle (white arrow).

Although interface is an important discriminator for differential diagnosis, focal fibrosis, organising pneumonia and mucin-producing tumour should be excluded. Focal fibrosis and organising pneumonia with a well-defined interface, which are caused by the alveolar septum thickening due to fibrosis and the air-containing space is similar to the MDCT manifestation of adenocarcinoma [22–24]. An ill-defined interface may occur in peripheral lung cancer, with an incidence of about 10%, which is an atypical presentation and mainly occurs in mucin-producing BAC. Mucin accumulation in the alveolar space around the tumour results in an ill-defined interface, which resembles inflammation.

The pleural indentation sign was also a common and valuable indicator for differential diagnosis of malignancy. The prerequisites of pleural indentation include the following two aspects: no conglutination between the parietal pleura and visceral pleura, and a distance between of lesion and pleura >2 cm. Based on these prerequisites, the contraction of fibrous tissue inside the lesion leads to pleural indentation [20, 25]. The frequency of pleural indentation was significantly higher in malignant fGGOs than in benign fGGOs (70.5% *vs* 4.8%). In addition, it mainly occurred in mGGOs. Nambu et al [18] hypothesised that it may be attributed to the strong contraction of the solid component.

The frequency of spiculation, spine-like process, bronchus cut-off, other air-containing space and vascular convergence in malignant fGGOs was significantly higher than in benign fGGOs, though they are not the important risk factors for malignancy. Moreover, no spine-like process or bronchus cut-off was observed in benign fGGOs. It is therefore assumed that either spine-like process or bronchus cut-off might be specific for malignancy. With respect to the demographic data, lesion size, location and attenuation value, no differences were found between benign and malignant fGGOs, which is consistent with previous studies [11, 19, 26].

There are several limitations in the present study, which suggests that further investigation is warranted. First of all, with regard to case selection, the sample size of benign fGGOs was small, especially for pGGO; the follow-up duration was relatively short; and most of the benign fGGOs were diagnosed according to size reduction or complete disappearance of the lesion as evidenced by the anti-inflammatory therapy. However, some benign and many malignant fGGOs with long volume-doubling time may remain unchanged in size and attenuation value even over a long follow-up period. In the present study, two lesions manifested stability during the follow-up period and are still being followed up, which were excluded from our study owing to their equivocal nature. Therefore,

Table 4. Binary logistic regression analysis of focal ground-glass opacity

Independent variables and constant	Variables in the equation							
							Exp(B) 95% CI	
	B	SE	Wals	df	Sig	Exp(B)	Lower	Upper
Lobulation	2.095	0.854	6.018	1	0.014	8.122	1.524	43.301
Interface	1.144	0.490	5.448	1	0.020	3.139	1.201	8.200
Pleural indentation	2.206	1.180	3.492	1	0.062	9.076	0.898	91.736
Constant	−2.268	0.790	8.246	1	0.004	0.103		

B, regression coefficient; CI, confidence interval; df, degrees of freedom; Exp(B), e^B=odds ratio; SE, standard error; Sig, significance; Wals, χ^2 value.

more cases and longer follow-up period are needed in future studies to obtain more accurate results. Also, the reconstruction parameters and window settings were the same for all fGGOs, which may result in possible missing features, especially for small pGGOs. So different reconstruction parameters and multiple middle window settings should be applied in future studies to take the size and attenuation value of fGGOs into consideration.

In conclusion, an fGGO nodule with lobulation, a well-defined but coarse interface and pleural indentation gives a greater than average likelihood of being malignant.

Acknowledgment

The authors would like to thank Professor Wei-hua Dong (Second Military Medical University) for critical reading and polishing the English language of the manuscript.

Reference

1. Sone S, Takashima S, Li F, Yang Z, Honda T, Maruyama Y, et al. Mass screening for lung cancer with mobile spiral computed tomography scanner. Lancet 1998;351:1242–5.
2. Henschke CI, McCauley DI, Yankelevitz DF, Naidich DP, McGuinness G, Miettinen OS, et al. Early Lung Cancer Action Project: overall design and findings from baseline screening. Lancet 1999;354:99–105.
3. Tsubamoto M, Kuriyama K, Kido S, Arisawa J, Kohno N, Johkoh T, et al. Detection of lung cancer on chest radiographs: analysis on the basis of size and extent of ground-glass opacity at thin-section CT. Radiology 2002;224:139–44.
4. Austin JH, Müller NL, Friedman PJ, Hansell DM, Naidich DP, Remy-Jardin M, et al. Glossary of terms for CT of the lung: recommendations of the Nomenclature Committee of the Fleischner Society. Radiology 1996;200:327–31.
5. Nakajima R, Yokose T, Kakinuma R, Nagai K, Nishiwaki Y, Ochiai A. Localized pure ground-glass opacity on high resolution CT: histologic characteristics. J Comput Assist Tomogr 2002;26:323–9.
6. Park CM, Goo JM, Lee HJ, Lee CH, Chun EJ, Im JG. Nodular ground-glass opacity at thin-section CT: histologic correlation and evaluation of change at follow-up. Radiographics 2007;27:391–408.
7. Hara M, Oda K, Ogino H, Oshima H, Sato Y, Kiriyama M, et al. Focal fibrosis as a cause of localized ground glass attenuation (GGA): CT and MR findings. Radiat Med 2002;20:93–5.
8. Kim HY, Shim YM, Lee KS, Han J, Yi CA, Kim YK. Persistent pulmonary nodular ground-glass opacity at thin-section CT: histopathologic comparisons. Radiology 2007;245:267–75.
9. Nakata M, Saeki H, Takata I, Segawa Y, Mogami H, Mandai K, et al. Focal ground-glass opacity detected by low-dose helical CT. Chest 2002;121:1464–7.
10. Aoki T, Nakata H, Watanabe H, Nakamura K, Kasai T, Hashimoto H, et al. Evolution of peripheral lung adenocarcinomas: CT findings correlated with histology and tumor doubling time. AJR Am J Roentgenol 2000;174:763–8.
11. Li F, Sone S, Abe H, MacMahon H, Doi K. Malignant versus benign nodules at CT screening for lung cancer: comparison of thin-section CT findings. Radiology 2004;233:793–8.
12. Henschke CI, Yankelevitz DF, Mirtcheva R, McGuinness G, McCauley D, Miettinen OS, et al. CT screening for lung cancer: frequency and significance of part-solid and nonsolid nodules. AJR Am J Roentgenol 2002;178:1053–7.
13. Yu H, Liu SY, Li HM, Xiao XS, Dong WH. Empirical description of bronchial and nonbronchial arteries with MDCT. Eur J Radiol 2010;75:147–53.
14. Cui Y, Ma DQ, Liu WH. Value of multiplanar reconstruction in MSCT in demonstrating the relationship between solitary pulmonary nodule and bronchus. Clin Imaging 2009;33:15–21.
15. Lee HJ, Goo JM, Lee CH, Yoo CG, Kim YT, Im JG. Nodular ground-glass opacities on thin-section CT: size change during follow-up and pathological results. Korean J Radiol 2007;8:22–31.
16. Jang HJ, Lee KS, Kwon OJ, Rhee CH, Shim YM, Han J. Bronchioloalveolar carcinoma: focal area of ground-glass attenuation at thin-section CT as an early sign. Radiology 1996;199:485–8.
17. Kim TJ, Goo JM, Lee KW, Park CM, Lee HJ. Clinical, pathological and thin-section CT features of persistent multiple ground-glass opacity nodules: comparison with solitary ground-glass opacity nodule. Lung Cancer 2009;64:171–8.
18. Nambu A, Araki T, Taguchi Y, Ozawa K, Miyata K, Miyazawa M, et al. Focal area of ground-glass opacity and ground-glass opacity predominance on thin-section CT: discrimination between neoplastic and non-neoplastic lesions. Clin Radiol 2005;60:1006–17.
19. Oh JY, Kwon SY, Yoon HI, Lee SM, Yim JJ, Lee JH, et al. Clinical significance of a solitary ground-glass opacity (GGO) lesion of the lung detected by chest CT. Lung Cancer 2007;55:67–73.
20. Winer-Muram HT. The solitary pulmonary nodule. Radiology 2006;239:34–49.
21. Zerhouni EA, Stitik FP, Siegelman SS, Naidich DP, Sagel SS, Proto AV, et al. CT of the pulmonary nodule: a cooperative study. Radiology 1986;160:319–27.
22. Ujita M, Renzoni EA, Veeraraghavan S, Wells AU, Hansell DM. Organizing pneumonia: perilobular pattern at thin-section CT. Radiology 2004;232:757–61.
23. Yang PS, Lee KS, Han J, Kim EA, Kim TS, Choo IW. Focal organizing pneumonia: CT and pathologic findings. J Korean Med Sci 2001;16:573–8.
24. Park CM, Goo JM, Lee HJ, Lee CH, Chung DH, Chun EJ, et al. Focal interstitial fibrosis manifesting as nodular ground-glass opacity: thin-section CT findings. Eur Radiol 2007;17:2325–31.
25. Kuriyama K, Tateishi R, Doi O, Kodama K, Tatsuta M, Matsuda M, et al. CT-pathologic correlation in small peripheral lung cancers. AJR Am J Roentgenol 1987;149:1139–43.
26. Ohtsuka T, Watanabe K, Kaji M, Naruke T, Suemasu K. A clinicopathological study of resected pulmonary nodules with focal pure ground-glass opacity. Eur J Cardiothorac Surg 2006;30:160–3.